Quaternary International 519 (2019) 58–73

Contents lists available at ScienceDirect

Quaternary International

journal homepage: www.elsevier.com/locate/quaint

Tologoi key section: A unique archive for pliocene-pleistocene paleoenvironment dynamics of Transbaikalia, Bikal rift zone

V.V. Ivanova[a,b,*], M.A. Erbajeva[b,c], A.A. Shchetnikov[b,d,e], A. Yu Kazansky[f,g], G.G. Matasova[i], N.V. Alexeeva[c], I.A. Filinov[c,d,e]

[a] FSBI "VNIIOkeangeologia", Russian Federal Subsurface Resources Agency (Rosnedra), Saint-Petersburg, Russia
[b] Vinogradov Institute of Geochemistry, Russian Academy of Sciences, Irkutsk, Russia
[c] Geological Institute, Siberian Branch Russian Academy of Sciences, Ulan-Ude, Russia
[d] Institute of the Earth's Crust, Siberian Branch, Russian Academy of Sciences, Irkutsk, Russia
[e] Irkutsk Scientific Centre, Siberian Branch, Russian Academy of Sciences, Irkutsk, Russia
[f] Faculty of Geology, Lomonosov Moscow State University, Russia
[g] Geological Institute, Russian Academy of Sciences, Moscow, Russia
[i] Institute of Petroleum Geology and Geophysics, Siberian Branch, Russian Academy of Sciences, Novosibirsk, Russia

ARTICLE INFO

Keywords:
Tologoi key section
Transbaikal region
Siberia
Pliocene
Pleistocene
Geology
Geochemistry
Grain size analysis
Lithology
Paleoenvironment
Biostratigraphy

ABSTRACT

The multi-layered key section of Tologoi is situated on the Selenga River left bank, 15 km southwest of Ulan-Ude city (51°45′ N, 107°29' E), in the Western Transbaikal region. It holds a long record of Quaternary sedimentation since early Late Pliocene through Holocene, with the only minor gap in the beginning of Early Pleistocene. Comprehensive studies have been carried out on the lithology, geochemistry, fauna succession and paleoenvironment reconstructions. This paper summarizes the data acquired on the geology and stratigraphy of the Tologoi section. The authors investigated the composition, structure and formation conditions of the section, as well as the intensity of weathering, rock geochemistry, grain size and biostratigraphy.

1. Introduction

The multi-layered key section Tologoi is situated on the Selenga River left bank, 15 km southwest of Ulan-Ude city (51° 45′ N, 107° 29' E) in the western Transbaikal region (Fig. 1). Stretching at 51°-56° N and 104°-118° E, the study area is located in the Baikal rift zone enclosed within Central Asia. It is noteworthy that this region experienced complicated geological evolution through the Pliocene and Pleistocene time. This region is known for diversity of landscapes: the territory covers deep intermountain depressions alternated by mountain ranges, their altitudes varying from 1000 m in the south to over 2600 m in the north. The North-Asian Arctic boreal areas are covered with mountainous taiga and meadows, deep forests and intermountain meadow-steppes being common for the semiarid landscapes. The Central-Asian arid landscapes with mountainous and dry steppes are available as well.

The extremely continental climate is typified by considerable amplitudes of both daily and annual temperature fluctuations. The mean January temperatures commonly vary from −20° to −30 °C, absolute minimum reaches −45°. In summer time, the mean July temperature is about 20 °C, absolute maxima range from 35° to 38°. As to the precipitation rates, they are typically low both in winter and in summer. Remarkably that in the Baikal region the weather is predominantly sunny and bright during winter time. In general, the climate is characterized by a negative mean annual air temperature (−1.25 °C). The annual precipitation is 250–400 mm (Sochava, 1967).

The Tologoi Key Section, discovered by Okladnikov A.P. in 1951, presents a sequence of continental deposits which had accumulated in the Ivolga depression since Late Pliocene through the Holocene, with the only minor gap in the beginning of Early Pleistocene. Primary information on this study area and its fauna was given by Bibikova et al. (1953).

Although the intensive investigations on geology of the Tologoi

* Corresponding author. Institute for Geology and Mineral Resources of the Ocean (VNIIOkeangeologia), Angliiskiy pr., 1, St. Petersburg, 190121, Russia.
E-mail addresses: vargeo66@gmail.com (V.V. Ivanova), erbajeva@ginst.ru (M.A. Erbajeva), shch@crust.irk.ru (A.A. Shchetnikov), kazansky_alex@mail.ru (A.Y. Kazansky), MatasovaGG@ipgg.sbras.ru (G.G. Matasova), octohona@online.ru (N.V. Alexeeva), filinov@crust.irk.ru (I.A. Filinov).

https://doi.org/10.1016/j.quaint.2018.11.004
Received 30 March 2018; Received in revised form 1 November 2018; Accepted 7 November 2018
Available online 10 November 2018
1040-6182/

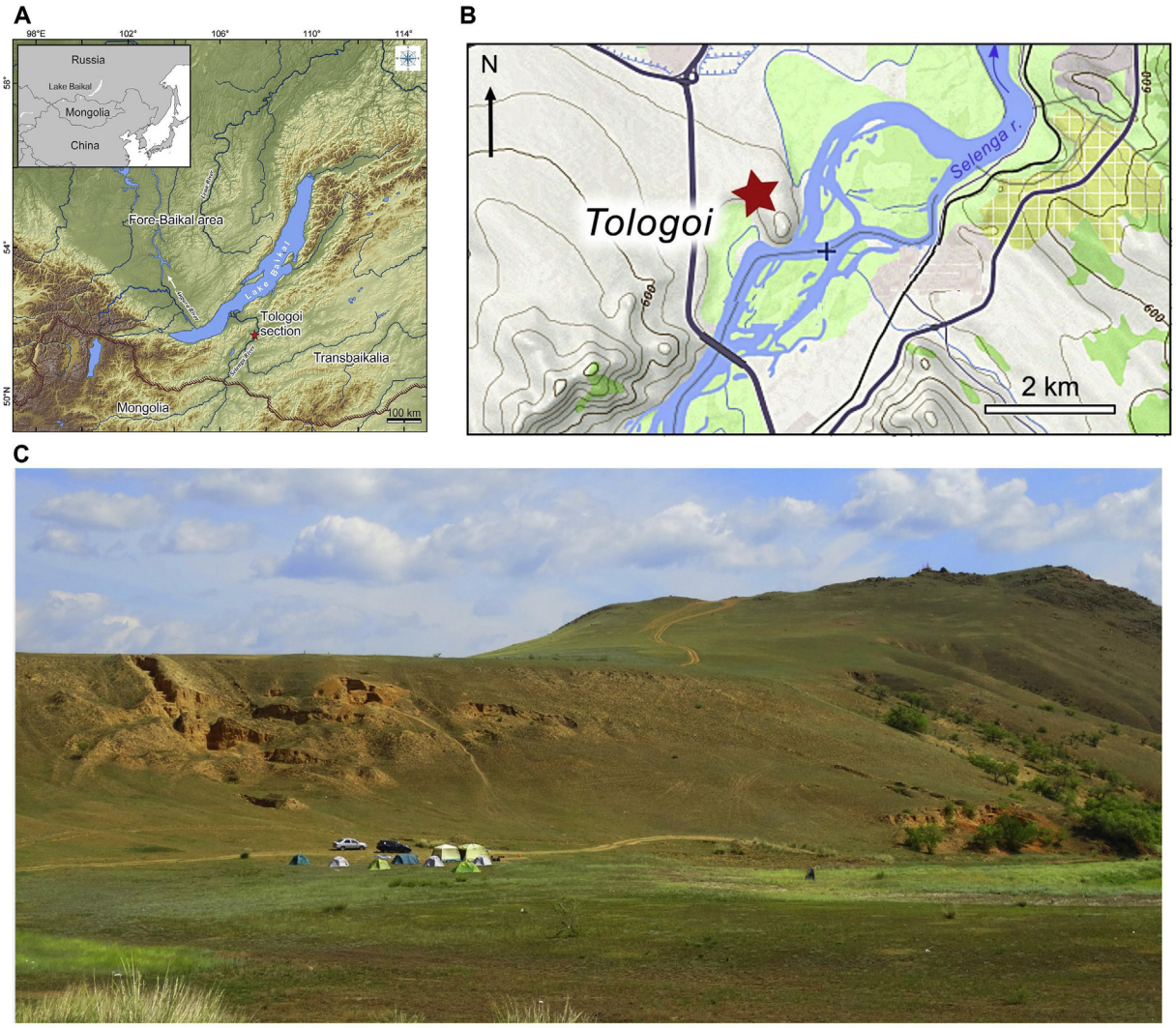

Fig. 1. General map with location of the studied area showing the Tologoi Key section (A); the location of the Tologoi Key section on the left bank of the Selenga river (B), the photograph of the section at Tologoi (Photo by Filinov I.A.) (C).

locality and its fauna are still in progress, acquired results seem fairly significant for paleoenvironment reconstructions and biostratigraphy not only for the Transbaikal, but for the entire Baikal region.

The Tologoi section contains the stratigraphic types of the Tologoi fauna complex and the Ivolga fauna, as well as the stratigraphic type of Tologoi (= Chikoy) Formation (Logatchev et al., 1964; Ravsky et al., 1964; Vangengeim et al., 1966; Bazarov, 1968; Erbajeva, 1970; Erbajeva, Alexeeva, 2000; Alexeeva, 2005; Erbajeva et al., 2005).

In the section, the magnetostratigraphy has been studied for the first time, and fossil remains have been recovered from both under and above the Matuyama/Brunhes reversal (Gnibidenko et al., 1976; Alexeeva, 2005). The earliest permafrost evidence in the Western Transbaikal region (dated as Early Pleistocene) was also found in this section (Vogt et al., 1995; Alexeeva, Erbajeva, 2000). However, Bazarov (1968) and Ravsky (1972) previously assumed that permafrost appeared in the Transbaikal region in the Riss time.

Cooperation with Prof. W. Zech (Germany, Bayreuth) provided new information on the Holocene and Late Pleistocene fossil soil structure and data on fossil formation. The sediments and fossil soil were dated (Zech et al., 2017). Moreover, the lithology, geochemistry, fauna succession and paleoenvironment reconstructions have recently been surveyed in detail. This work is mainly targeted at reporting acquired results.

2. Materials and methods

The Tologoi Key section was studied with multidisciplinary approaches, e.g. the geological structure was analyzed using lithological, granulometric and mineralogical methods; and the geochemical method was first tried in this research. When describing the color of sediments, the properties of the Munsell Soil Color Chart are used (describing color by hue, value, and chroma). Paleontological data are based on newly acquired results and detailed revision of previously gained materials. Fossil mammal remains have been recovered from nearly 13 fauna horizons proving successive fauna development from the Late Pliocene through Holocene time.

In our study we followed the Standard Chronostratigraphy meaning that the Pliocene/Pleistocene boundary is at 2.588 Ma as suggested by the IUGS chart (Pillans, Gibbard, 2012; Cohen, Gibbard, 2016).

To analyze granulometric composition of sediments of the Tologoi section 222 samples have been collected at spacing 10 cm at complete profile of the section. Granulometric composition was measured by laser micro analyzer of particles Microtrac X100. The size of measured particles ranges from 704 μm to 0.146 μm, which for convenience were united into 50 fractions given for each sample in volume percent. Samples were disintegrated via ultrasonic treatment.

The results on all samples were statistically processed with program GRADISTAT (Blott, Pye, 2001). Each sample was characterized by the

modes of distribution, average grain size, sorting, asymmetry and eccentricity. The results of measurements for statistical analysis were united by fractions of fragments and particles into sand fraction (> 100 μm), coarse silt (50–100 μm), fine silt (10–50 μm) and clay (< 10 μm), according to classification by A.V. Raukas (1981). The calculations were performed by the method of arithmetic moments (Gradzin'skii et al., 1980) and Folk- Ward method (Folk, Ward, 1957) modified by Blott and Pye (Blott, Pye, 2001), providing more precise values for the total granulometric characteristics of a sample. Some additional calculation parameters were applied as well.

- F – is the dynamic factor representing the ratio of physical sand amount (sum of fractions > 50 μm) to the amount of physical clay (sum of fractions < 50 μm) in a sample. The parameter characterizes sedimentation conditions: with F > 1 there prevails the clastic material inflow from the neighboring and middle sources by dragging and saltation (~to ten kilometers), that most likely takes place in highly-dynamic medium at strong fitful winds; with F < 1 the clastic material inflow diminishes, and it arrives as air aerosols, basically from remote sources; there prevail post-sedimentation transformations of sediments *in situ*, causing soil formation;
- K – is the indicator of dispersion reflecting the features of clay components. It is commonly applied for specifying such phenomena as getting characteristics of podzol- and clay-like soils due to transformation, transfer and localization of finely dispersed substance in different sediments. It is calculated (Berezin, 1983) as:

$$K = (\ln C_5 - \ln C_1)/1.609$$

where C_5 – content of particles (%) with diameter < 5 μm; C_1 – contents of particles (%) with diameter < 1 μm; ln – natural logarifm (a logarithm with *e* as a base).

To identify the geochemical composition of the Tologoi sediments the petrochemical analyses (222 samples collected at spacing 0.1 m and complete profile of section) were performed for the terrigenous rocks. The contents of rare and dispersed elements (Li, Ba, Sc, Cu, Zn, Co, Ni, Y, Nb, Cs, Th, U) were determined in the rocks by XRF technique at the Institute of the Earth's Crust, SB RAS, Irkutsk. The contents of rock-forming element oxides were determined by the «wet chemistry» method. The REE (rare earth elements) contents were measured in 20 samples (sampling spacing varies depending on the particle size distribution from 0.2 to 2.6 m) with relative error 5–10% by ICP-MS at the Institute of Geochemistry SB RAS, Irkutsk. Analytical results were statistically treated with the Statistica 10.0 software.

In order to obtain the general characteristics of rocks of the Tologoi Key section, we analyzed the distribution of some geochemical proxies (LOI, P_2O_5, Cu, Zn and Co) and the main petrochemical indices and pedogenic ratios (listed in Table 1) across the section (222 samples).

In order to determine the degree of weathering we used the following weathering proxies: chemical index of alteration CIA = $(Al_2O_3/(Al_2O_3 + CaO + Na_2O + K_2O))*100$ (Nesbitt, Young, 1982), chemical index of weathering CIW = $(Al_2O_3/(Al_2O_3 + CaO + Na_2O))*100$ (Fedo et al., 1995), index of compositional variability ICV = $(Fe_2O_3 + K_2O + Na_2O + CaO + MgO + TiO_2)/Al_2O_3$ (Cox et al., 1995); index of the plagioclase transformation degree PIA = $((Al_2O_3 - K_2O)/(Al_2O_3 + CaO + Na_2O - K_2O))*100$ (Fedo et al., 1995);

To disclose the behavior of Rare Earth Elements during weathering and pedogenesis, we applied the REE signature diagrams - patterns of NASC-normalized (Gromet et al., 1984) REE concentrations, which allow comparing the concentration, distribution, and the degree of REE fractionation in each sample. Then, the geochemical differences between the sediments were searched with the following criteria often used in various REE studies on sedimentary rocks:

- value of Ce and Eu anomaly, expressed as $Ce^* = 3Ce_n/(2La_n + Nd_n)$

Table 1
Petrochemical indices and pedogenic ratios.

Index	Calculation	Proxy information	Pedogenic process	Reference
HM	$\frac{(Al_2O_3 + TiO_2 + Fe_2O_3 + FeO + MnO)}{SiO_2}$	Hydrolizate index. Intensity of chemical weathering	Hydrolysis	Yudovich, Ketris (2000); Maslov (2005);
TM	$\frac{TiO_2}{Al_2O_3}$	Titanium index. Ti is most readily removed by physical weathering, Al by chemical weathering. Acidification (provenance)	Acidification	Yudovich, Ketris (2000); Maslov (2005); Sheldon (2006)
SM	$\frac{Na_2O}{Al_2O_3}$	Sodium index. Intensity of chemical weathering: degradation of plagioclases.	Alkali elements accumulate as soluble salts not removed: salinization	Yudovich, Ketris (2000); Maslov (2005); Retallack (2007)
AM	$\frac{Na_2O}{K_2O}$	Alkaline index. The ratio is a signal of the K-feldspar and mica content versus plagioclase content in the sediments.	Salinization	Yudovich, Ketris (2000); Maslov (2005); Retallack (2007)
NAM	$\frac{(Na_2O + K_2O)}{Al_2O_3}$;	Normalized alkalinity index. Prevalence of feldspars. Provenance (presence of basic volcanic rocks)-high values.	Salinization	Yudovich, Ketris (2000); Maslov (2005); Retallack (2001); Sheldon and Tabor (2009)
ASM	$\frac{Al_2O_3}{SiO_2}$	Alumosilicic index. Degree of weathering. Clayeyness. Al accumulated as clay minerals form	Hydrolysis	Yudovich, Ketris (2000); Maslov (2005); Sheldon and Tabor (2009)
A/CMNK	$Al_2O_3/(CaO + Na_2O + K_2O + MgO)$	Common rock-forming alkaline and alkaline earth elements are lost relative to Al during pedogenesis	Hydrolysis	Retallack (2007); Grazhdankin, Maslov (2012)
$\frac{(CaO + MgO)}{Al_2O_3}$	$\frac{(CaO + MgO)}{Al_2O_3}$	The ratio reflects the accumulation of soil calcite and dolomite	Calcification	Retallack (2007)
Ba/Sr	$\frac{Al_2O_3}{Ba/Sr}$	Sr solubility > Ba solubility	Leaching, hydrolysis	Retallack (2001); Sheldon and Tabor (2009)
$\frac{(Fe_2O_3 + MnO)}{Al_2O_3}$	$\frac{(Fe_2O_3 + MnO)}{Al_2O_3}$	The ratio reflects the sedimentation redox conditions. High values characterize oxidizing environment	Redox conditions	Kalinin et al. (2009)

(Taylor and McLennan, 1985) and Eu* = $2Eu_n/(Sm_n + Gd_n)$ (Balashov, 1976);
- Σ(REE + Y) – the total content of REE and yttrium (Balashov, 1976); ΣLREE, ΣMREE and ΣHREE-content of the light (La–Nd), middle (Sm–Dy) and heavy (Er–Lu) rare earth elements, respectively.
- ΣCe/ΣY, where ΣCe (La–Gd), ΣY(Tb–Lu, Y) is an indicator of how intense erosion processes are (Balashov, 1976);
- La/Yb, La/Sm - indicators of the facies sediment accumulation conditions (Trueman et al., 2006);

As an additional criterion of changes in the LREE/HREE abundance the magnitude of the tetrad effect of lanthanide fractionation was used for the 3rd and 4th tetrads, T3 and T4 (Monecke et al., 2002). The tetrad effect is the spectrum infraction of REE concentrations normalized by NASC, expressed in splitting the entire spectrum into groups (tetrads) with formation of a zigzag-shaped line: La–Ce–Pr–Nd, Pm–Sm–Eu–Gd, Gd–Tb–Dy–Ho, and Er–Tm–Yb–Lu. For each tetrad in the REE spectrum curves are formed with the boundaries between Nd and Sm, on Gd and between Ho and Er (McLennan, 1994). The tetrad effect can be treated similarly to the quantification of Ce or Eu anomalies in logarithmic representations (Irber, 1999) as equation (1):

$$ti = \sqrt{\frac{v1 \times v4}{v2 \times v3}} \quad (1)$$

in which v_1, v_2, v_3 and v_4 are the normalized concentrations of 1st, 2nd, 3rd and 4th lanthanide in each individual tetrad.

The concave segments of the tetrad exhibit the W– type effect, whereas convex segments exhibit the M-type. In a solution, the W-type effect results from the complex REE compound foundation, equilibrium with the colloidal hydroxyl compounds Fe and Mn, and the presence of slightly reduced conditions (Dia et al., 2000). The W-type tetrad effect is detected in sea water, ground water, as well as limestones and other sedimentary rocks (Masuda, Ikeushi, 1979; Masuda et al., 1987). The W-type tetrad effects are found significant as 0.9; for M-type tetrad effect the values over 1.1 are significant.

Monecke et al. (2002) reported that the size of the tetrad effect of a single tetrad in the logarithmic REE plot is better described by the standard deviation of normalized concentrations of two central elements (v2 and v3) within the tetrad from a straight line connecting the contents of the first (v1) and the last element (v4) and proposed mathematical expressions to quantify the tetrad effect. The size of the tetrad effects in normalized distribution patterns is calculated for all the tetrad groups symbolized as T_i (i = 1, 2, 3, and 4) (equation (2)):

$$Ti = \sqrt{\frac{1}{2} \times \left(\left(\frac{v2}{\sqrt[3]{v1^2} \times \sqrt[3]{v4}} \right) - 1 \right)^2 + \left(\left(\frac{v3}{\sqrt[3]{v1} \times \sqrt[3]{v4^2}} \right) - 1 \right)^2} \quad (2)$$

in which v_1, v_2, v_3 and v_4 are the normalized concentrations of the 1st, 2nd, 3rd and 4th lanthanide in each individual tetrad.

Thus, $T_i = 0$ means that all elements of each tetrad group lie on the straight line. The value of the tetrad effect for the first tetrad should not be quantified in case of significant Ce anomaly. Calculation of the value of the tetrad effect for the 2nd tetrad is impossible, because Pm is not available in nature (McLennan, 1994).

The value of the tetrad effect is significant, when $T_i > 0.2$, whereas the t_i values calculated by equation (1) have to be below 0.9 for the concave, and higher than 1.1 for the significant convex tetrad effects.

The magnitude of the tetrad effect (Irber, 1999; Monecke et al., 2002) of lanthanide fractionation was employed for the 3rd and 4th tetrads (T3, T4) as an additional criterion for geochemical analysis (Ivanova et al., 2016) of the exposure.

The classification diagrams and behavior of the indices and tetrad effects described above according to the sediment deposition order were analyzed to partition the geochemical exposure.

For soil horizons of the Tologoi section the geochemical data was attracted to reconstruct paleo temperatures and mean annual amount of precipitation (Sheldon, Tabor, 2009).

The dependences of geochemical indices on the mean annual level of atmospheric precipitation and temperature are described by equations (3) and (4):

$$P = -130.93 \times \ln(CaO_{molar}/Al_2O_{3molar}) + 467.4 \quad (3)$$

$$T = -18.516 \times ((Na_2O_{molar} + K_2O_{molar})/Al_2O_{3molar}) + 17.298 \quad (4)$$

3. Paleoenvironment background

In Early Pliocene, the tectonic uplift of the mountain, surrounding Lake Baikal, produced the major orographic barrier separating the Transbaikal region from the influence of the western humid Atlantic cyclones (Prokopenko et al., 2001; Kuzmin, Yarmoluyk, 2006). This uplift seems to be the main reason for generating aridization conditions in the Transbaikal region. The Late Pliocene warm and semiarid climate changed to cooler and arid climate. The savanna-like forests and steppes gradually reduced, and were replaced by the open landscapes, mainly diverse steppes. The climate was still warm and became moderately arid (Erbajeva et al., 2013). At the Early Pleistocene the global cooling was registered in the Northern Hemisphere. In the Baikal region, the cold intervals were recorded at the stage 2.82–2.5 Ma (Prokopenko et al., 2001). The further intensive cooling of the Early Pleistocene was registered in the Baikal region at the time interval 1.75–1.45 Ma, when Alpine glaciers existed in the higher mountains, while low mountains, foothills and valley floors were underlain by permafrost. Significant reorganizations occurred in the fauna assemblages and paleo flora. In the Transbaikal region in the mammal faunas the Central Asian elements predominated as in contemporaneous faunas of China and Mongolia (Alexeeva, Erbajeva, 2005; Erbajeva et al., 2013).

At the beginning of the Middle Pleistocene the progressive cooling caused significant reorganization in the paleoenvironment and biota of Transbaikal region, the climate became cooler and drier. This time interval is distinguished by high aridity of climate and predominance of inhabitants of the desert, semi-desert and dry steppes; small mammal faunas resemble the recent fauna in southern Mongolia (Alexeeva, Erbajeva, 2005; Erbajeva et al., 2013).

Toward the Late Pleistocene time, the paleoenvironment changed and became more or less periglacial. Dry steppes with prevailing wormwood plants widely expanded through the Transbaikal region. Most of small mammals reminded of currently existent species; however the distribution area of some species extended deeply to the North-East, far beyond their present habitats (Alexeeva et al., 2014).

4. Geological setting

Exposed in the Tologoi locality, the Late Pliocene-Holocene sediments are widely distributed throughout the Transbaikal region. All the researchers involved in the study of Tologoi section agree in distinguishing three sedimentary units in the sequence: Tologoi 1, Tologoi 2 and Tologoi 3 (Fig. 2 A). The successive fossil soils are present in three units (Ravsky et al., 1964; Bazarov, 1968; Vangengeim et al., 1966; Erbajeva, 1970; Alexeeva, 2005).

The lower UNIT deposits (Tologoi 1 section) belong to the Tologoi (= Chikoy) Formation and it is exposed on 3.0 m. The sediments accumulated at the earliest stage of Late Pliocene. They have a reversed polarity and belong to the Gauss Chron (Gnibidenko et al., 1976). The exposed profile exhibits two different color beds separated by a horizon of calcareous concretions: upper part consists of red sandy clay with abundant debris, and the lower part includes reddish and dark brown loam (paleosoil) (Fig. 2 B). Fossil remains of small mammals are found in both beds, above and below the calcareous concretion horizon, and they slightly differ by the evolutionary stages of species. The fauna of

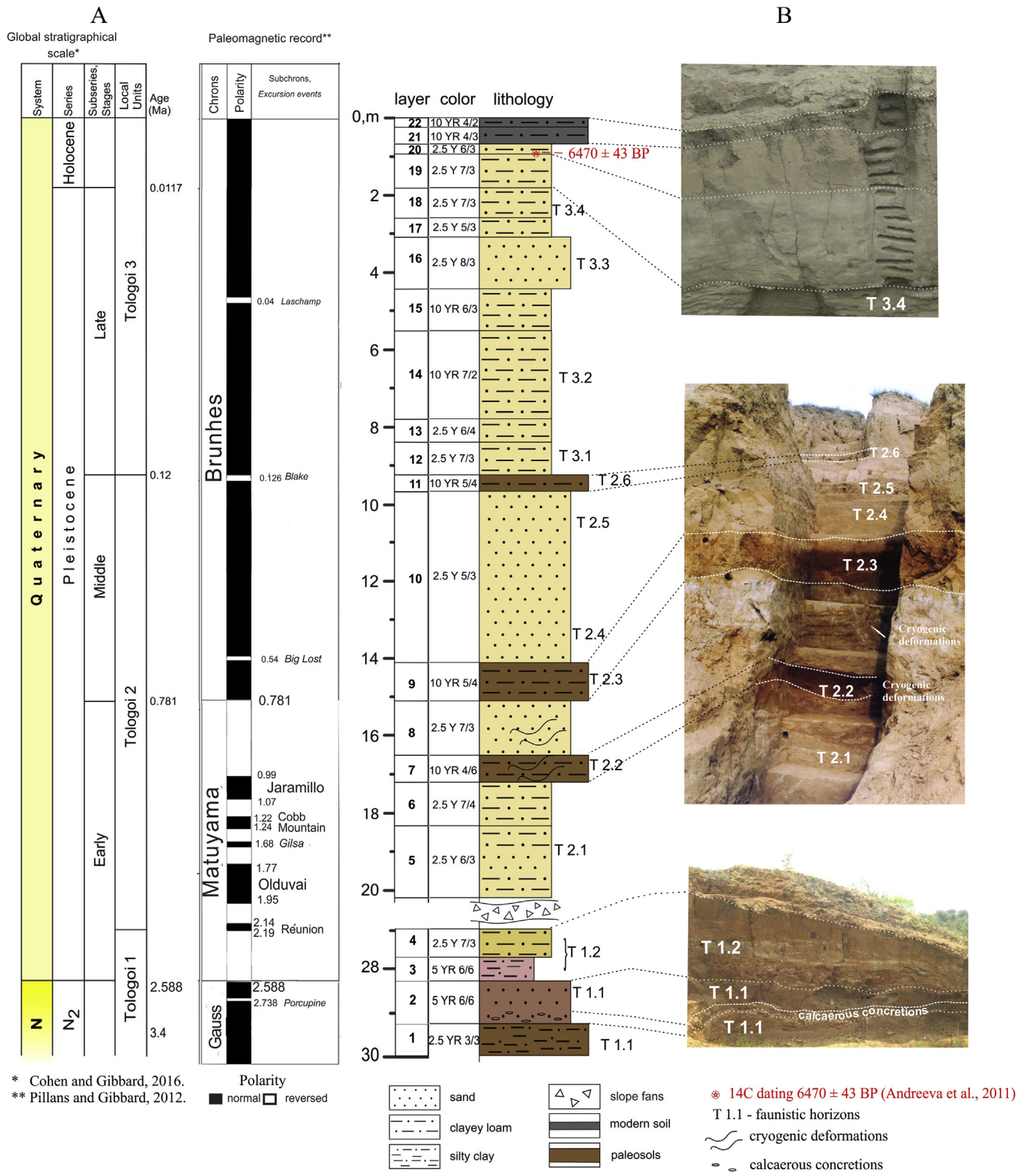

Fig. 2. Chronostratigraphy and lithology of the Tologoi section (A). Photographs of the Tologoi Key section, showing the position of faunistic horizons (B). Photo by Erbajeva M. A.

both horizons belong to the Chikoy Faunistic complex (Erbajeva et al., 2005), it is the Tologoi 1.1 fauna.

The red beds are overlain by erosional unconformity of pinkish, reddish-yellow-grey loam holding sand and occasionally concretions and laminas of carbonate up to 1 m thick. It contains scarce remains of the Early Pleistocene Dodogolian fauna (Tologoi 1.2 fauna) (Erbajeva et al., 2005). This pinkish-color horizon is traced upwards by the yellowish-grey and brownish sandy loam up to 0.6 m thick. Scarce fossils of the late Early Pleistocene period are contained in the sediments. Above this pinkish-color horizon, the sediments were characterized by

the yellowish-grey and brownish sandy loam up to 0.6 m thick.

The middle UNIT (Tologoi 2 section**)** is approximately 12 m thick. It is composed of unsorted compact pale-yellow, pale-greyish and brownish sandy loam, with occasional grains of coarse sand and small lenses of fine gravel up to 1.5 m thick. The sediments of this unit belong to the Ivolga Formation (Erbajeva et al., 2005). This section contains three fossil soil horizons: upper, middle and lower.

In the middle part of the section the Matuyama-Brunhes magnetic reversal occurs within of the middle fossil soil horizon (Gnibidenko et al., 1976).

The lowermost part (2.5 m) of the section lying below the Matuyama-Brunhes boundary is affected by cryogenic deformations (see Fig. 2 B). The deformations were discovered in the lower fossil soil. These cryogenic structures are dated to the interval between 0.78 and 0.99 Ma, as they are located below the Matuyama-Brunhes boundary, though above the positive Jaramillo event (Alexeeva, Erbajeva, 2000).

It is the earliest permafrost evidence dated to the Early Pleistocene in the Western Transbaikal region. In this part, below the reversal, two successive small mammalian faunas attributed to the late Early Pleistocene (faunas of Tologoi 2.1 and Tologoi 2.2) have been recovered.

The lower fossil soil horizon is overlain by the fine-sandy loam (1.4 m thick) which also contains cryogenic crack (80 cm deep, 60 cm wide at the top) and smaller diverse-sized cracks (wedges) banded with calcareous dust.

The horizon above consists of the red-brownish sandy loam. It is the second (middle) fossil soil of the Tologoi 2 section. Dated as Middle Pleistocene, three mammal faunas were discovered (faunas of Tologoi 2.3, 2.4 and Tologoi 2.5). They belong to the Tologoi Faunistic complex.

The sequence of the Tologoi 2 section is capped by the brownish loamy deposits, referred to the upper fossil soil horizon.

The upper UNIT (Tologoi 3 section) 9–10 m thick overlies the erosional surface of the sediments of the middle unit Tologoi 2. The sediments of Tologoi 3 consist of unsorted yellow-grey and brownish sandy loam admixed with fine gravel and sand. They belong to the Krivoyarsky Formation The sediments are coarser than those of the underlying middle unit. In the upper unit at least three cycles of sedimentation with cryogenic deformations are traced. The evidence of cold stage is present as diverse periglacial features, as a variety of solifluction flow, thick carbonate interlayers and short small cracks. There are scarce remains of small mammals from 4 levels (T 3.1, T 3.2, T 3.3, T 3.4 faunas) attributed to the Late Pleistocene time. Ravsky et al., 1964 and Bazarov (1968), who previously studied the section, suggested a Late Pleistocene age for the uppermost part of Tologoi 3. However, the Holocene age of this fossil soil was confirmed by ^{14}C dating as 6470 ± 43 BP (Andreeva et al., 2011).

5. Paleontology and biostratigraphy

Fossils of the earliest stage are derived from the beds below the calcareous concretion horizon in the lower unit (Tologoi 1 section). They belong to *Hypolagus* sp.; *Ochotonoides complicidens* Boule et Teilhard de Chardin, 1928; *Ochotona* sp.; *Cricetinus* cf. *varians* Zdansky, 1928; *Promimomys* cf. *stehlini* Kormos, 1931; *Cseria gracilis* Kretzoi, 1959; *Mimomys* cf. *minor* Feifar, 1961; *Villanyia* cf. *eleonorae* Erbajeva, 1975; *Mesosiphneus praetingi* Teilhard de Chardin, 1942 (Alexeeva, 2005). These fossils characterize the earliest stage of Tologoi 1.1 fauna.

The mammal remains from the red sediments above the calcareous concretion horizon are: *Beremendia fissidens* Petenyi, 1864; *Petenyia hungarica* Kormos, 1930; *Sorex* sp.; *Hypolagus multiplicatus* Erbajeva, 1976; *Hypolagus transbaicalicus* Erbajeva (1970); *Ochotonoides complicidens; Ochotona intermedia* Erbajeva, 1976; *Orientalomys sibiricus* Erbajeva, 1976; *Cricetinus* cf. *varians; Cricetulus* cf. *barabensis* Pallas, 1773; *Kowalskia* sp.; *Mimomys* cf. *minor; Mimomys.* cf. *reidi* Hinton, 1910; *Villanyia eleonorae, Pitymimomys koenigswaldi* Erbajeva, Alexeeva, Khenzykhenova (2005); *Pliosiphneus* aff. *lyratus* Teilhard de Chardin, 1942; *Mesosiphneus praetingi* (Erbajeva, Alexeeva, 2000; Alexeeva, 2005). These fossils characterize the youngest stage of Tologoi 1.1 fauna.

The species composition shows that faunas of these two stages differ essentially in the taxa composition and evolutionary level of arvicolids. This fact indicates the variety of the paleoenvironment conditions during the formation of sediments of this unit. The fauna characterizes the climate as warm and semiarid; the savanna-like landscapes prevailed in the region (Alexeeva, 2005).

The Late Pliocene Tologoi 1.1 fauna is followed with gap by the Early Pleistocene Tologoi 1.2 fauna attributed to the Dodogolian one and containing *Borsodia laguriformes* (Erbajeva, 1973), *Allophaiomys deucalion* Kretzoi, 1961, *Episiphneus youngi* Teilhard de Chardin et Young, 1931, *Ochotona bazarovi* Erbajeva, 1988, and *Spermophilus tologoicus* Erbajeva et Pokatilov, 1966.

The following Early Pleistocene biostratigraphic stage is featured by the pale-yellow, pale-greyish and brownish sandy loam of the Ivolga Formation exposed in the middle unit of the Tologoi Key section. The Tologoi 2 section is approximately 12 m thick. Three fossil soils within this profile and six successive faunas of small mammals have been identified in this unit. Moreover, in the middle of this unit the Matuyama/Brunhes reversal occurs within fossil soil horizon. It should be stressed that below paleomagnetic reversal some lines of evidence on cryogenic deformations were observed in the section that demonstrates cool and arid conditions. The lowermost bed was found to contain small mammal fauna of the Kudinian faunal stage; it includes: *Crocidura* sp.*; Ochotona tologoica* Habaeva, 1958; *Ochotona* cf. *sibirica* Erbajeva, 1988; *Spermophilus tologoicus*; *Allactaga* sp.; *Allophaiomys pliocaenicus* Kormos, 1932; *Prolagurus* cf. *pannonicus* Kormos, 1930; *Eolagurus* sp.; *Episiphneus* ex gr. *youngi; Lasiopodomys* sp. (Alexeeva, 2005). The fauna is common for widely distributed open landscapes with meadow steppes and lowland meadows; the climate was cool, but became slightly humid.

The next biostratigraphic stage of the Tologoi profile yielded for the Middle Pleistocene fauna of Tologoi complex which includes: *Ochotona gureevi* Erbajeva, 1966; *Marmota nekipelovi* Erbajeva, 1966; *Spermophilus gromovi* Erbajeva, 1966; *Cricetulus* cf. *barabensis; Allactaga sibirica transbaikalica* Erbajeva, 1966; *Ellobius tancrei* Blasius, 1884; *Meriones unguiculatus* Milne-Edwards, 1867; *Eolagurus simplicidens* Young, 1934; *Myospalax wongi* Young, 1934; *Lasiopodomys brandti* Radde, 1861; *Microtus gregalis* Pallas, 1779; *Microtus mongolicus* Radde, 1861. The dominant forms are the Central Asian taxa inhabiting dry steppes, semideserts and deserts. It indicates the extremely dry environment during that period and rather cool climate. Therefore, that period is believed to have the driest conditions in the Transbaikal region.

The following Middle Pleistocene Ivolginian fauna (T 2.6) includes: *Ochotona daurica* Pallas, 1776; *Eolagurus* cf. *luteus* Eversmann, 1840*; Marmota sibirica* Radde, 1862; *Allactaga* sp.*; Spermophilus undulatus* Pallas, 1778; *Lagurus lagurus* Pallas, 1773; *Lasiopodomys brandti* (Alexeeva, 2005). The species composition suggests that open landscapes still exist with dry steppe and patches of subdesert. The climate was sharp continental, relatively cold and semiarid.

In the stratigraphic sequence the Late Pleistocene stage is characterized by the deposits of the upper unit (Tologoi 3) consisting of yellow-grey and brownish sandy loam admixed with fine gravel and coarse sand.

Four faunistic horizons (T 3.1 – T 3.4) were recognized in this unit, three of them - the Late Pleistocene and uppermost one of the Holocene (^{14}C dating 6470 ± 43 BP - Andreeva et al., 2011). Thus, the Late Pleistocene fauna consists of: *Ochotona daurica; Marmota sibirica; Spermophilus undulates; Cricetulus barabensis; Lagurus lagurus; Clethrionomys rufocanus* Sundevall, 1846; *Lasiopodomys brandti; Microtus gregalis*. Some characteristic elements are common for the periglacial landscapes. It is noteworthy, that the faunas of cold and warm periods were not very much distinguished by the species composition due to arid climate, however they differ in their quantitative correlations.

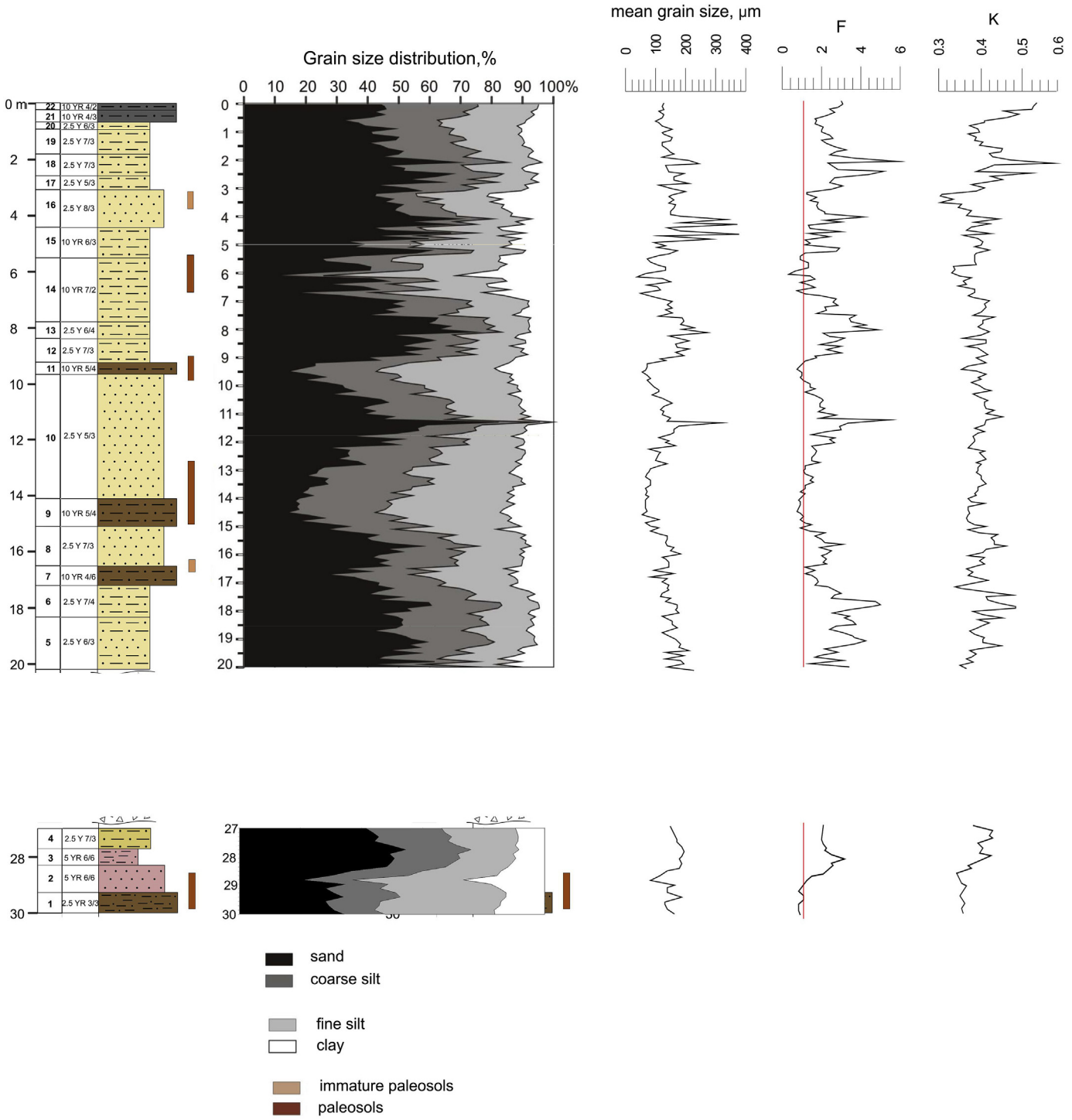

Fig. 3. Granulometric composition of sediments of Tologoi section. F – dynamic factor, D_{mean} – mean size of grain, K – index of sediment dispersion. Red line marks the "border" value of factor F (equal 1). The brown color to the right of the lithology column marks the paleosols horizons established by granulometric data. The legend to the lithology column is shown on Fig. 2. (For interpretation of the references to color in this figure legend, the reader is referred to the Web version of this article.)

The Holocene fauna mostly includes the modern species.

6. Results

6.1. Grain size analyses

Fig. 3 presents variation of all granulometric parameters with depth. The study of granulometric data allowed to refine the thicknesses and to indicate specific characteristics of some layers. The formal parameter for recognition is dynamic factor F, which is the ratio of physical sand (the sum of sand and coarse silt fractions) content to physical clay (the sum of fine silt and clay fractions) content. Its values < 1 (or closer to 1) point to the predominance of secondary post-sedimentation processes and slowdown of eolian sedimentary material supply. Decrease of dispersion coefficient K indicates localization of fine-dispersed material.

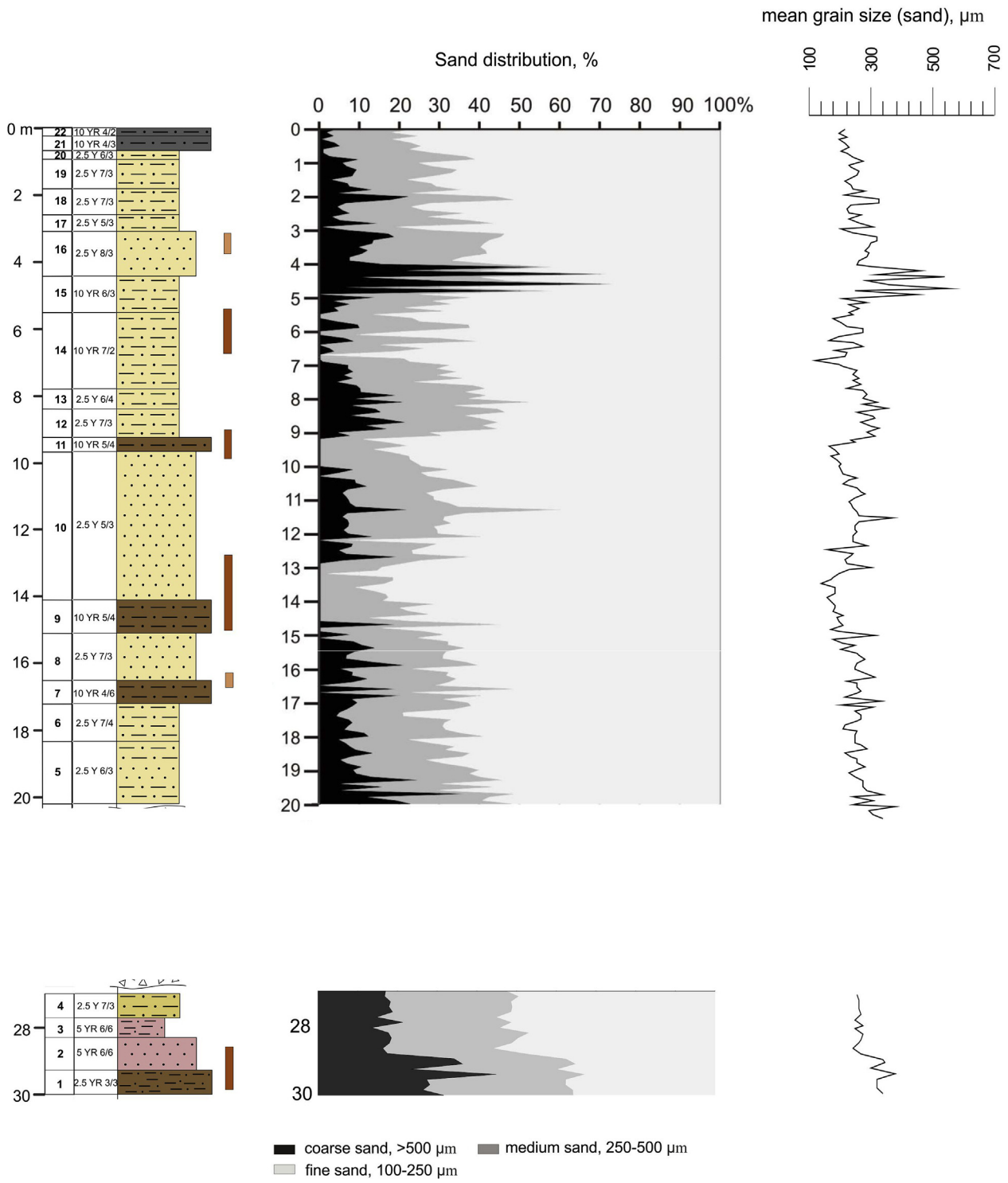

Fig. 4. Composition of sand fraction of sediments and mean grain size (sand).

The granulometric data point to the existence of 6 fossil soils: upper (depth 320–380 cm) one may be attributed to immature, fossil soil at 1650–1680 cm depth - to poorly preserved soil. Three paleosol horizons in the middle part of the section (Tologoi 2 unit) are clearly observed and have the significant thickness. The geological description recognizes 4 low buried soils; the granulometric data present the record on a slight displacement of boundaries (from 10 to 30 cm) and larger thickness of soil horizons. The point for discussion is the layer at depth 550–690 cm (Tologoi 3 unit, upper part of the section) having higher (relative to the other layers) content of clay fraction, reduction of mean grain size, decreased value of dispersion index K and value of dynamic factor F < 1. All these parameters are comparable with those in fossil soils at depth 910–990 cm and 1290–1500 cm.

With regard to a combination of granulometric indices, the intervals of mostly coarse-grained sediments have been recognized at 200–300 cm, 400–480 cm, 700–900 cm and 1130 cm. In the lower part of section, from depth 1540 cm the average grain size increases monotonously, except for the soil horizon.

As the sediments (not the buried soils) contain 40–80% of sand fraction (> 100 μm) and from 65 to 95% of physical sand (sum of

Table 2
Statistical features of the distribution of major oxides, LOI (%) and trace elements (ppm) in the Upper Cenozoic sediments of the Tologoi section (222 samples).

Elemental oxides and trace elements	Mean	Median	Min	Max	Std. Dev.[a]	Coef. var., %[b]
SiO_2	65.5	65.6	56.5	72.4	2.7	4
TiO_2	0.6	0.6	0.3	0.9	0.2	26
Al_2O_3	14.7	14.8	13.0	16.1	0.7	5
Fe_2O_3	2.5	2.3	0.9	4.3	0.7	29
FeO	1.0	1.0	0.3	1.5	0.2	22
MnO	0.1	0.1	0.0	0.1	0.0	31
MgO	1.3	1.2	0.5	2.3	0.4	29
CaO	3.7	3.4	1.2	12.8	1.5	41
Na_2O	3.3	3.3	2.5	3.9	0.2	6
K_2O	3.8	3.7	2.6	5.0	0.5	15
P_2O_5	0.2	0.2	0.1	0.4	0.0	27
LOI	1.9	1.8	0.4	3.5	0.6	32
CO_2	1.1	0.7	0.1	9.1	1.2	103
V	44.6	42.0	24.0	72.0	10.9	24
Cr	8.7	8.0	2.0	101.0	6.7	77
Co	19.9	19.0	12.0	34.0	5.2	26
Ni	19.4	18.0	8.0	30.0	3.5	18
Cu	42.8	38.0	21.0	80.0	14.0	33
Zn	23.0	23.0	18.0	31.0	1.9	8
Rb	10.9	10.0	8.0	31.0	3.3	3
Sr	25.0	25.0	15.0	38.0	4.9	20
Nb	104	110	81	170	15	13
Cs	3.2	2.8	2.1	5.4	1.0	30
Ba	592	585	325	910	97	16
Hf	2.3	2.3	1.3	4.6	0.8	35
Ta	2.1	2.0	0.7	4.1	0.9	40
Th	5.7	5.0	3.0	30.2	3.1	21
U	866	905	400	1340	174	18

[a] Standard deviation.
[b] Coefficient of variation.

Table 3
Statistical features of the distribution of the petrochemical indices*.

Petrochemical indices	Mean	Median	Minimum	Maximum	Std.Dev.	Coef.var.,%
HM	0.29	0.28	0.22	0.37	0.03	10
TM	0.04	0.04	0.02	0.06	0.01	24
ASM	0.23	0.23	0.19	0.26	0.01	6
SM	0.22	0.23	0.18	0.26	0.02	7
NAM	0.48	0.49	0.35	0.60	0.05	10
AM	0.88	0.88	0.61	1.11	0.11	13

* For the legend see Table 2. For the petrochemical indices see Table 1.

Table 4
Statistical features of the distribution of the weathering proxies*.

Weathering proxies	Mean	Median	Minimum	Maximum	Std.Dev.	Coef.var., %
CIA	55.7	55.1	48.8	78.5	3.9	7
CIW	65.3	64.3	58.9	81.0	4.1	6
ICV	1.0	1.0	0.8	1.9	0.1	13
PIA	57.0	57.3	48.1	66.9	3.4	6

* For the legend see Table 2. For the weathering proxies see Chapter Materials and Methods.

coarse-silt and sand fractions), it makes sense to consider separately the composition of sand fraction: content of fine-grained (100–250 μm), medium-grained (250–500 μm) and coarse-grained sand (> 500 μm) (Fig. 4).

The supposed intervals of buried soils largely contain fine-grained sand, and most samples do not contain coarse-grained sand, except for the uppermost poorly developed soil. It is evident from the distribution of sand fractions, that the pattern is preserved and becomes even more distinct.

6.2. Geochemistry

Major and trace element composition of the Tologoi section sediments is presented in Appendix (Supplementary Data). Statistical features of the distribution of major oxides, LOI (%) and trace elements in the Upper Cenozoic sediments of the Tologoi section are shown in Table 2.

Variability of petrochemical indices is presented in Table 3.

Variability of weathering proxies is shown in Table 4.

The trend of silicate and plagioclase weathering is displayed on the ternary diagrams Al_2O_3–(CaO + Na_2O)–K_2O (Nesbitt, Young, 1984) and CaO–(Al_2O_3-K_2O)–Na_2O (Fedo et al., 1995) (Fig. 5A and B).

Figs. 6–8 shows variation of all geochemical indices with depth.

To create a detailed geochemical division of the section we reviewed the distribution of geochemical indices (see Figs. 6–8). Position of horizons of fossil soils agrees with that identified through granulometric characteristics. The paleosol layer at depth 550–690 cm, which is distinguished from granulometric characteristics, is clearly observed in the geochemical profile.

The paleo temperatures and mean annual precipitation were reconstructed from the geochemical data for the Tologoi section fossil soils (Sheldon, Tabor, 2009, equations (3) and (4)) (Table 5).

Table 6 provides REE composition of the Tologoi section sediments.

The comparison of the normalized REE concentrations in the Tologoi section sediments (Fig. 9) indicates that REE distributions in all analyzed samples show common characteristics: excess of light lanthanides with the deficit of the heavy ones.

The La_N/Yb_N—La_N/Sm_N ratio obtained for the rocks of the section (Fig. 10) matches the continental (fluvial) sedimentation settings (Trueman et al., 2006).

Variations of geochemical coefficients indicate that for sediments of the Tologoi section mostly significant is fractionation of medium and heavy REEs (Fig. 11).

7. Discussion

7.1. Lithology

Acquired data pinpoint that sediments of the section primarily consist of sands, sandy loam and loam alternating cyclically, as shown in Fig. 3. The sedimentation cyclicity is mostly vivid on the plots of sand fractions (see Fig. 4). Cyclic recurrence results in the reduction of coarse sand supply, in some periods to zero, and increase of amount of this sand fraction to 20–30% (at depth 400–500 cm – to 70%) in the other periods. Four plotted cycles (Tologoi 2 and Tologoi 3 units) terminate with formation of soil horizons, including recent soil. The buried soil horizon in the lower part of the section (Tologoi 1 unit) (2900–3000 cm) reflects the end of sedimentation cycle. Considering grain size parameters, the upper segment of the section (Tologoi 2 and Tologoi 3 units) is divided into two parts; the boundary approximately runs through fossil soil at depth 900–950 cm. The upper layers are composed of poorly sorted sediments with a great variability of granulometric composition. The lower layers formed at a quieter behavior of sedimentation with grain size values gradually changing within layers. Most sediments show an average degree of sorting, and at depth 13–17 m the sediments look as well sorted. In general, through the section all soils (including recent soil) are more homogeneous in granulometric composition and, accordingly, they are better sorted than sand and sabulous sediments.

Average dispersion of clay components in the Tologoi section designated as coefficient K is 0.4. This value characterizes sediments composing the section as finely dusty and indicates poor development of soil-forming processes and predominant presence of chlorite-illite mineral group.

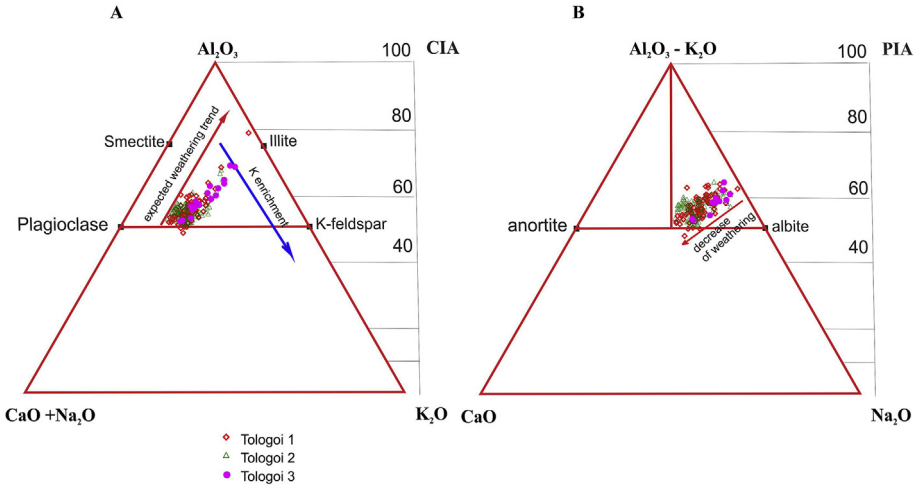

Fig. 5. Ternary diagrams exhibiting the trend of silicate and plagioclase weathering: (A) A-CN-K: (CaO + Na_2O)–Al_2O_3–K_2O diagram (Nesbitt and Young, 1984); (B) C-(A-K)-N: CaO–(Al_2O_3–K_2O)–Na_2O diagram (Fedo et al., 1995). Arrows indicate weathering trends.

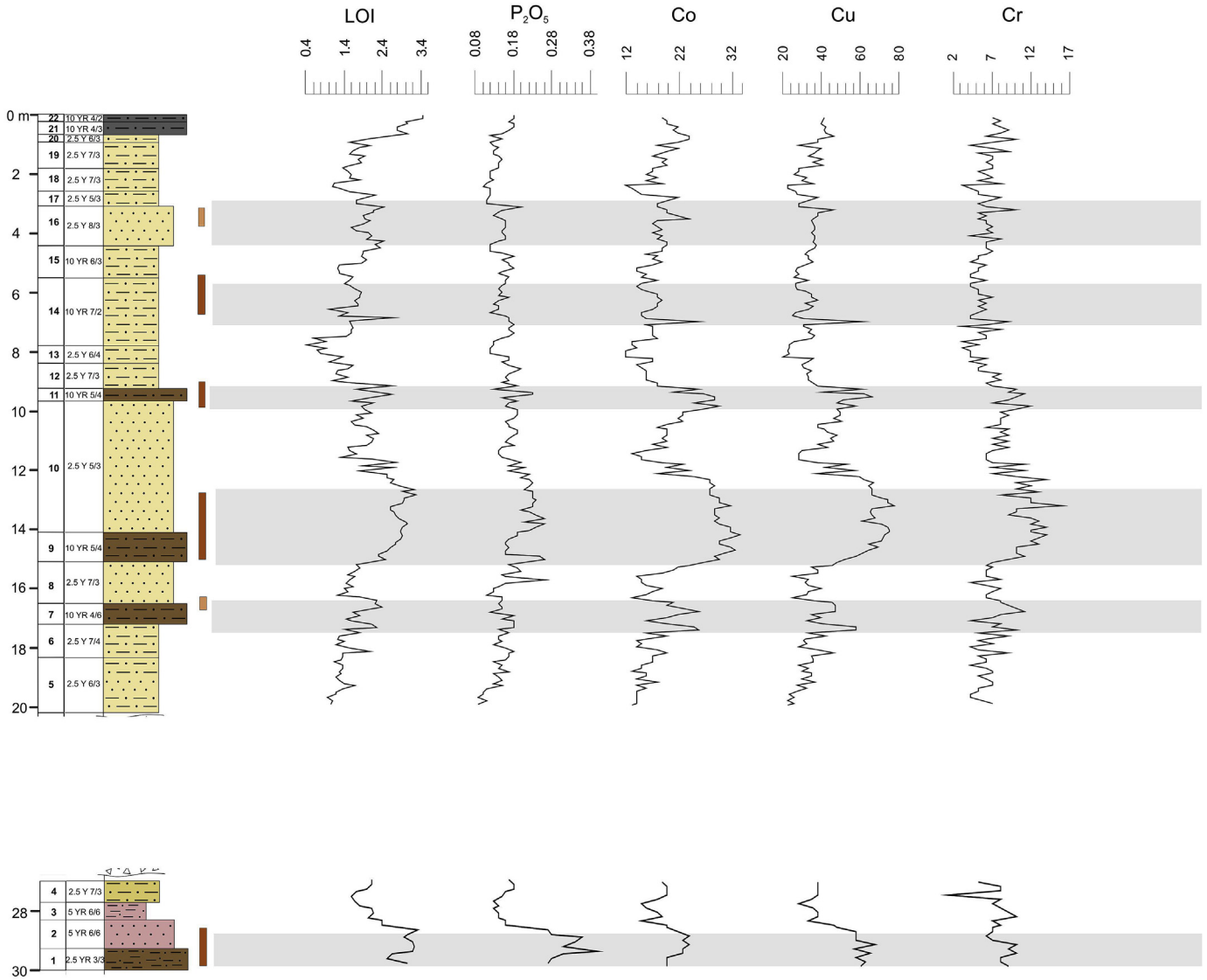

Fig. 6. Variation of the geochemical proxies along the depth profile. The brown color to the right of the lithology column marks the paleosols horizons established by granulometric data, the grey color - by geochemical data. The legend to the lithology column is shown on Fig. 2. (For interpretation of the references to color in this figure legend, the reader is referred to the Web version of this article.)

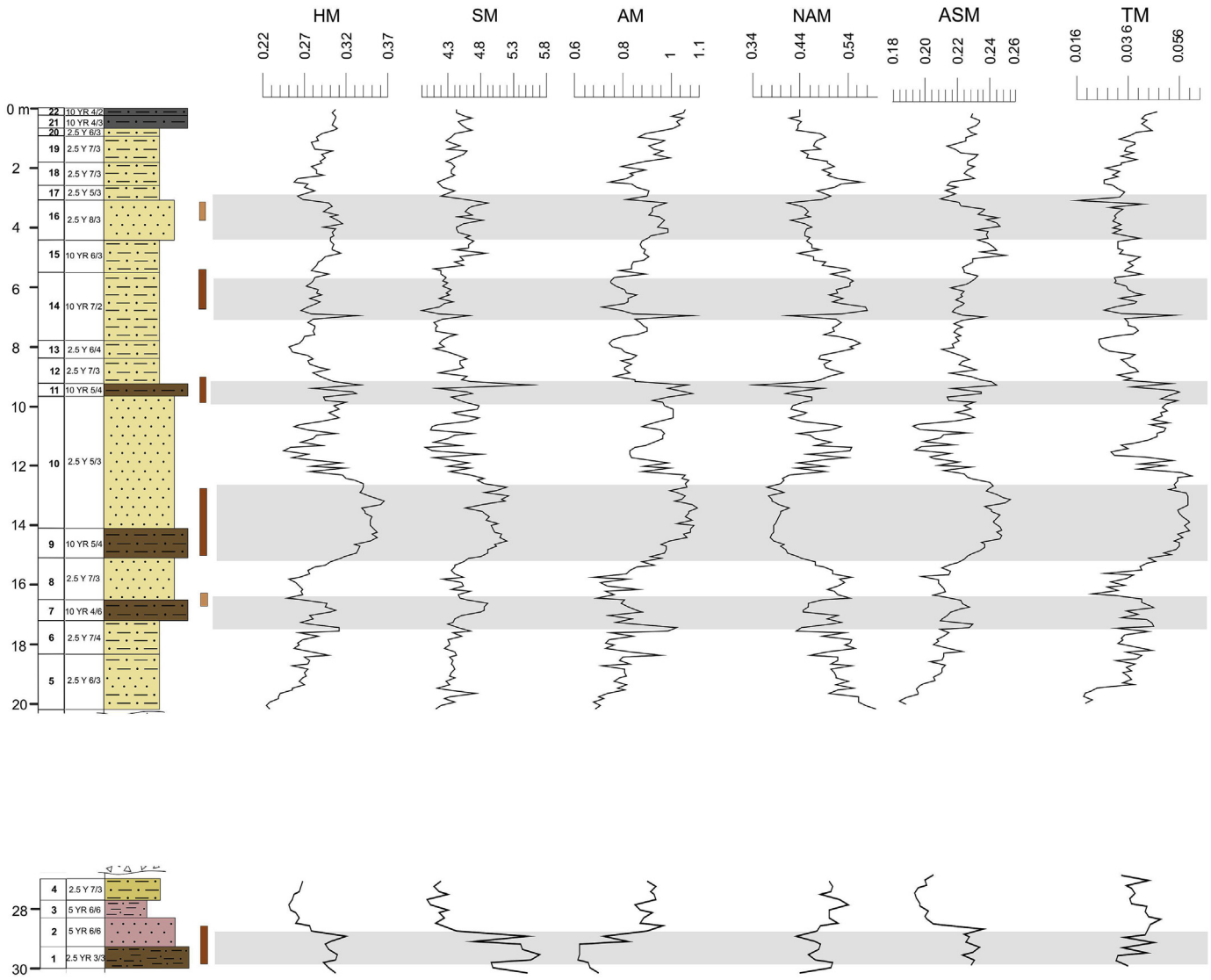

Fig. 7. Variation of the petrochemical indices along the depth profile. The brown color to the right of the lithology column marks the paleosols horizons established by granulometric data, the grey color - by geochemical data. The legend to the lithology column is shown on Fig. 2. (For interpretation of the references to color in this figure legend, the reader is referred to the Web version of this article.)

Thus, the granulometric analysis of sediments distinguished the following features of sedimentation in the Tologoi section:

- Cyclic sedimentation traced by the behavior of all fractions, but most vividly by varying sand content. Four key cycles were recognized within Tologoi 2 and Tologoi 3 units, each cycle terminated by the formation of soil horizons (pedocomplexes). The buried soil horizon in the lower part of the section (Tologoi 1 unit) (2900–3000 cm) reflects the end of sedimentation cycle;
- Most of the Tologoi Key section sediments have a complex granulometric composition represented by different grain populations. With the exception of buried soils horizons, sediments contain 40–80% of sand fraction (> 100 μm) and 65–95% of physical sand (sum of coarse-silt and sand fractions);
- Sedimentary material was transported to the sedimentation site basically from the nearby source; probably they were alluvial sediments of the Selenga River blown by strong winds. At the stages of warming and formation of soil horizons the wind flaws calmed down and thus the strength of wind flow reduced. Under these conditions, the remote and average-distance provenance of sedimentary material was primary. During intense pedogenic processes the sand material supply diminished, at times to zero (see Fig. 4), and biochemical post-sedimentation transformations of *in situ* sediments dominated;
- If granulometric features of sediments are believed to be climatically preconditioned, in this part of the Selenga River valley prevailed large-amplitude fluctuations of climate: from cold dry to hot dry conditions with minor changes toward increase of humidity in the periods of soil formation. It is highly probable that wind activity was quite intense producing strong hurricane flaws in the dry periods;
- Sediments composing Tologoi 2 unit (depth 10–20 m) formed in quieter wind conditions compared to the Tologoi 3.

7.2. Major and trace elements, loss on ignition and assessment of weathering

The analysis of bulk chemical composition of the Tologoi section sediments shows (see Table 2) minor variations of petrogenic oxide contents and trace elements, except for CaO, CO_2, Cr.

Variability of petrochemical indices (see Table 3) is not high, that is the evidence of genetic affinity of the sediment provenance. High values of AM and NAM indices (see Table 3), low values of HM point to

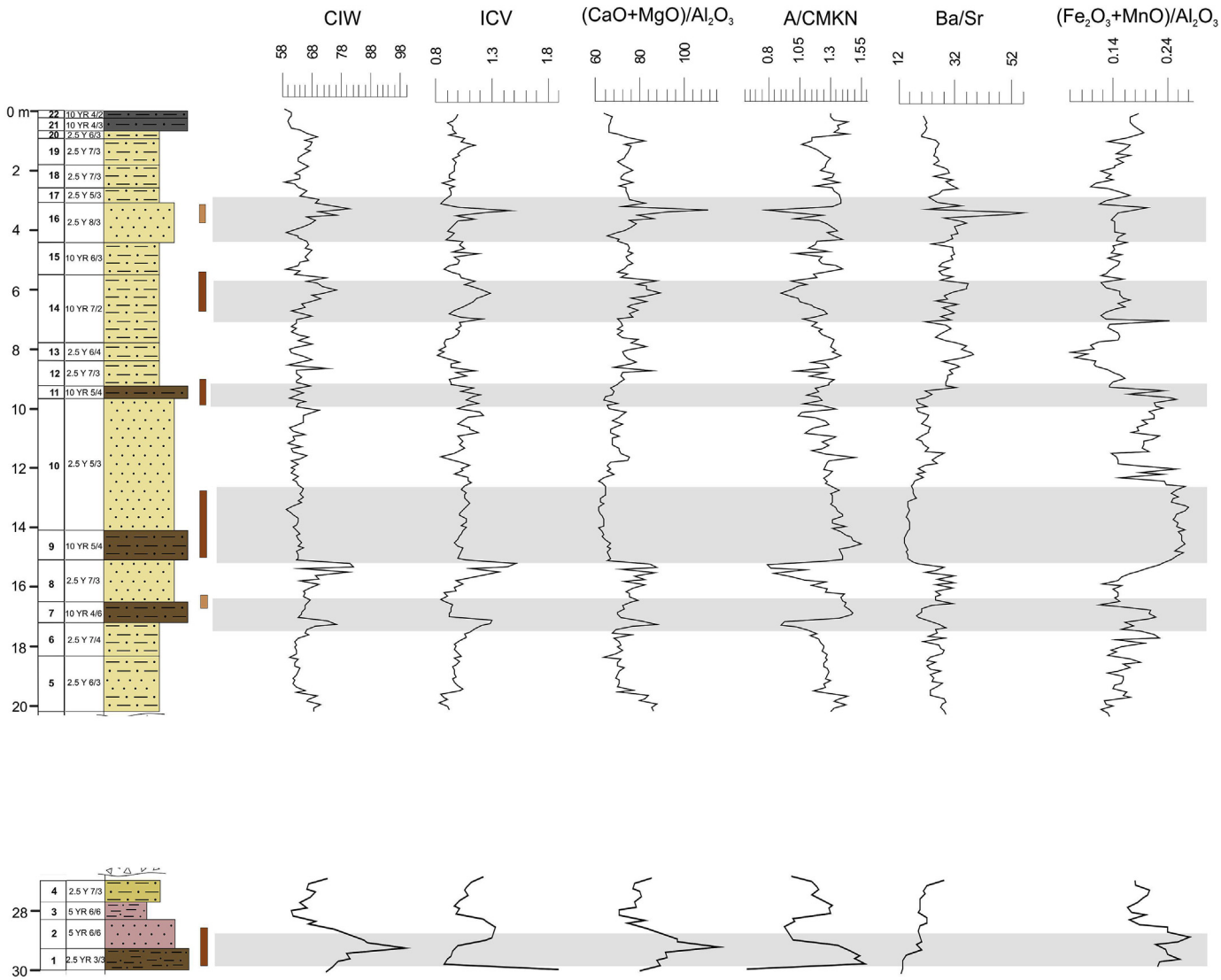

Fig. 8. Variation of the weathering proxies and pedogenic ratios along the depth profile. The brown color to the right of the lithology column marks the paleosols horizons established by granulometric data, the grey color - by geochemical data. The legend to the lithology column is shown on Fig. 2. (For interpretation of the references to color in this figure legend, the reader is referred to the Web version of this article.)

predominance in the initial sediments of quartz and feldspar with low content of clay minerals.

Considering the mean value of hydrolizate index (HM = 0.29), the studied sediments may be attributed to hypohydrolizates, i.e. poorly transformed by weathering processes. The sodium index SM reflects the intensity of chemical weathering and maturity of the material supplied to the sedimentation site. Low values of this index (0.01–0.02) characterize the high degree of chemical weathering at paleo catchment area (Yudovich, Ketris, 2000). The studied sediments show an extremely low level of chemical differentiation, the mean SM is 0.22 (see Table 3). The NAM values reach 0.4, it is the evidence on feldspar predominance in sediments. The range of PIA values (see Table 4) matches the subarid sedimentation settings.

The trend of silicate weathering is plotted on Al_2O_3–(CaO + Na_2O)–K_2O ternary diagram (Nesbitt, Young, 1984) (see Fig. 5 A). The cloud of points on the plot A-CN-K inclined toward K_2O vertice might indicate that sediments underwent potassium metasomatism at the stage of diagenesis. The cloud of points occur close to the «plagioclase – feldspar» line and below the «smectite-illite» line, indicating that feldspars dominate amongst Al–bearing minerals. The plagioclase trend of weathering is plotted on CaO–(Al_2O_3-K_2O)–Na_2O ternary diagram (Fedo et al., 1995) (see Fig. 5 B). Sediments cluster in the middle of the plot largely closer to the albite composition. Comparison of weathering trends for silicates and plagioclases reveals the evidence, that sediments of the Tologoi section predominantly contain feldspars. Climatic settings in the provenance areas were subarid.

The CIA values varying from 33 to 65 and low ICV values (Table 4) suggest arrival into the sedimentation area of immature eroded material of basic and acid magmatic rocks. The index of compositional variability ICV ranges through the section (see Fig. 8) fairly widely: e.g. from 0.82 to 1.90. However fine sediments have high values evidencing the increase of eolian accumulation (ICV values over 1 imply low rock maturity, i.e. minor amount of clay minerals in sedimentation area). The observed CIA indicates arid or subarid climatic settings in the erosion sites.

To assess paleoclimate, the TM index values have been analyzed. The TM distribution through section agrees with the change of granulometric composition of rocks, and with the change of CIW and ICV (see Fig. 7). The variations of coefficient through the section testify to accumulation of sediments of the lower part (Tologoi 1) under conditions of dry arid climate, and the middle part (Tologoi 2) under warmer climate with intensification of climate aridization in accumulation of

Table 5
Calculation of mean annual precipitation (P, mm) and temperatures (T, C) of the Tologoi fossil soils*.

Calculated values	Mean	Median	Minimum	Maximum	Std.dev.	Coef. var., %
fossil soil horizon 320–380 cm						
P	524	555	432	588	58	11
T	6	6	6	7	0.3	5
fossil soil horizon 550–690 cm						
P	548	532	480	641	44	8
T	4	4	3	7	0.8	19
fossil soil horizon 910–990 cm						
P	564	574	522	601	29	5
T	6	6	5	8	1.0	16
fossil soil horizon 1290–1500 cm						
P	611	613	586	651	19	3
T	7	7	6	8	0.4	6
fossil soil horizon 1650–1680 cm						
P	646	647	633	656	10	2
T	6	6	6	6	0.1	2
fossil soil horizon 2900–3000 cm						
P	619	635	503	702	83	13
T	6	6	6	6	0.3	4

* For the legend see Table 2.

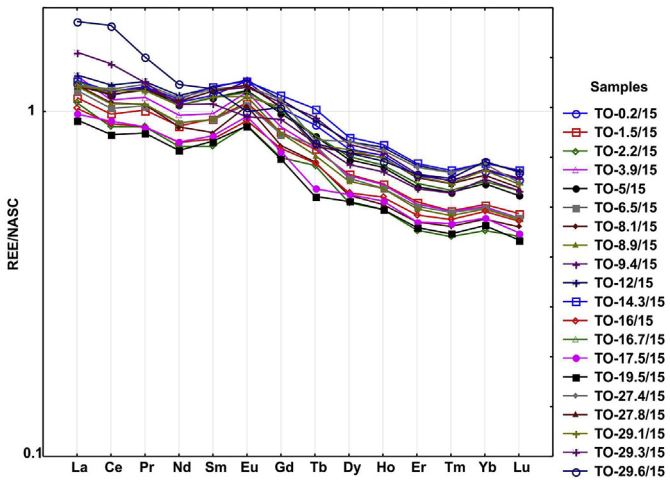

Fig. 9. NASC-normalized (Gromet et al., 1984) REE signatures in the sediments.

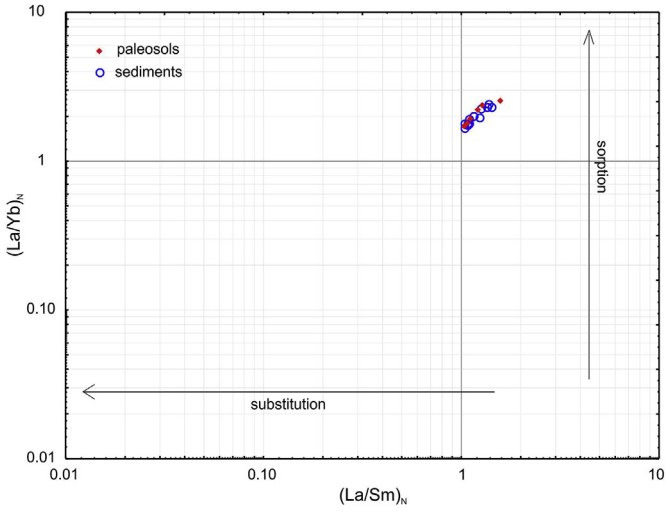

Fig. 10. Plot $(La/Yb)_N$ – $(La/Sm)_N$.

sediments of the upper part of the section (Tologoi 3).

Mean value of CIW in the studied sediments is 65; the proxy varies from 58 to 81, thus indicating insignificant level of rock alteration at paleo catchment area. The changes of CIW and ICV proceed synchronously, and the increase of CIW values with a simultaneous ICV decrease marks the periods of climate humidization.

The values of Al-Si index ASM (see Fig. 7), an indicator of clay mineral amount, vary from 0.19 to 0.26, giving proof on minor fractionation of material during transportation and its poor transformation in the process of weathering.

The variation of index A/CMKN (Fig. 8) indicates fossil soil horizons. Fossil soils are specified by increased values of index, due to weathering under conditions of periodic exsiccation (accumulation of Al_2O_3 and evacuation of Ca, Mg, Na and K oxides), as well as clay components and increased values of coefficient of soil material oxidation $(Fe_2O_3 + MnO)/Al_2O_3$. On the other hand, fossil soil horizons are distinguished by relatively low values of soil calcification index $(CaO + MgO)/Al_2O_3$, which is the evidence of carbonate phase outflow.

The sampled interval displays noticeable variations of petrogenic oxide contents corresponding to the sediments of different types. The sediments, which formed in the periods of relative warming, are characterized by increased concentrations of P_2O_5 (see Fig. 6).

The observed change of geochemical proxies LOI, Cu, Co, Cr, Ba/Sr (see Figs. 6 and 8) lets us to conclude that:

1) Increase of Cu, Co, Cr contents in sediments might be due to sorption of these elements by organic matter. High values of Ba/Sr in the fossil soil horizons prove development of processes of hydrolytic weathering.
2) The sharp changes of climate are characteristic for the middle part of the section (Tologoi 2 unit).

The acquired data pinpoint that climate in time of sediment formation changed cyclically: i.e. the periods of humidification were replaced by arid epochs of different intensity and duration. In particular, the most humid conditions and activation of weathering and leaching processes were identified in paleosol horizon at depth 1290–1500 cm and at depth 2900–3000 cm. Estimation of paleoclimatic characteristics (Table 5) records a gradual aridization of the climate in Transbaikalia during the Pleistocene. The obtained values mostly correspond with regional paleoclimatic reconstructions (e.g. Enikeev, 2008; Enikeev et al., 2013; Tarasov et al., 2009), but seem to be somewhat overestimated. According to paleontological data (Alexeeva, 2005), steppe landscapes dominated in the study area in the Middle and Late Pleistocene, requiring lower precipitation values.

7.3. Rare earth elements

As regards the REE sum, the Tologoi section rocks do no differ essentially, meaning low sedimentation rates (Balashov, 1976).

The Eu and Ce anomalies are indistinct. The value of index ΣCe/ΣY (mean 6.53) features the humid type of lithogenesis, but in this case it does not refer to the period of sediment formation; and because of insignificant chemical weathering it rather refers to the formation of source rocks.

The ΣCe/ΣY ratio decreases due to diminishing heavy lanthanoid mobility. Minor changes of some other geochemical ratios take place via poor chemical and mineral transformation of parent rocks at the early stages of weathering crust development.

Predominance of LREE over HREE is possibly the case owing to the presence of altered feldspar.

Comparison of plots of REE content distribution in the sediments (Fig. 9) offers some conclusions:

- REE spectra in general belong to the same type in all sediment

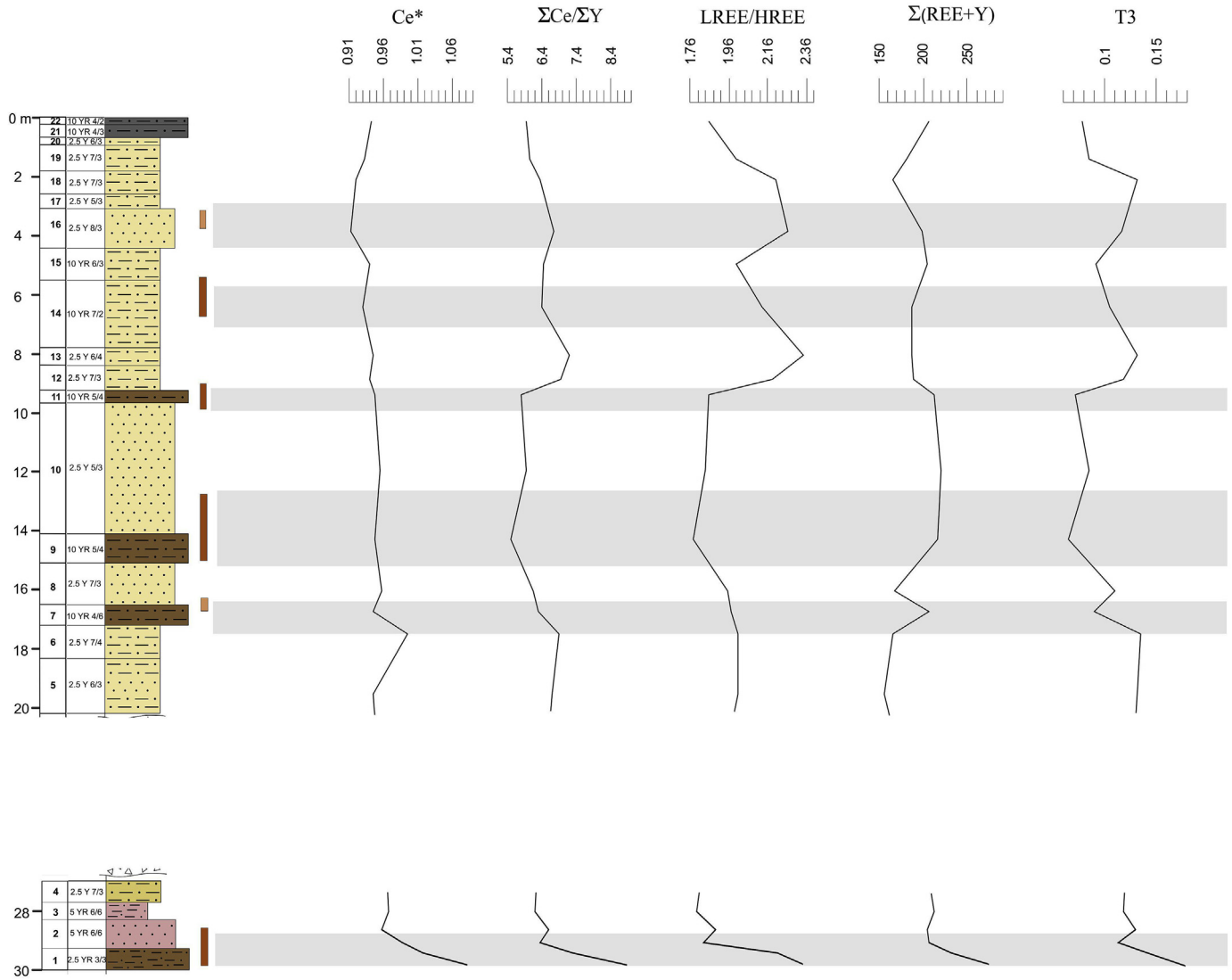

Fig. 11. Variations of indices reflecting REE fractionation with depth. The brown color to the right of the lithology column marks the paleosols horizons established by granulometric data, the grey color - by geochemical data. The legend to the lithology column is shown on Fig. 2. (For interpretation of the references to color in this figure legend, the reader is referred to the Web version of this article.)

Table 6
REE content and REE ratios in the Tologoi section sediments.*

REE content and REE ratios	Mean	Median	Minimum	Maximum	Std.dev.	Coef. var.%
Ce*	0.96	0.95	0.91	1.09	0.04	4
Eu*	1.12	1.13	0.91	1.25	0.09	8
LREE/HREE	2.02	2.00	1.77	2.36	0.19	9
ΣLREE	161.0	164	125.1	238.8	24.52	15
ΣMREE	17.0	18	13.4	20.1	2.23	13
ΣHREE	4.4	5	3.4	5.3	0.66	15
Σ(REE + Y)	199.6	204	154.9	280.2	28.01	14
ΣCe/ΣY	6.53	6.37	5.48	8.97	0.74	11
$(La/Yb)_N$	2.04	2.00	1.70	2.54	0.27	13
$(La/Sm)_N$	1.19	1.15	1.03	1.57	0.15	12
T3	0.11	0.12	0.06	0.18	0.03	25
T4	0.04	0.04	0.03	0.07	0.01	26
t3	0.95	0.95	0.89	1.00	0.03	4
t4	1.02	1.01	1.00	1.04	0.01	1

*For the legend see Table 2. Explanations for the REE content and REE ratios are given in the text (Chapter Materials and Methods).

samples. The excess of LREE and deficit of heavy ones are common for the sediments of continental runoff.
- studied rocks differ in the level of REE accumulation: e.g. the sediments in the lower part of the section have higher REE content.

Acquired $(La/Yb)_N$ –$(La/Sm)_N$ ratio (Fig. 10) represents the continental (fluvial) settings of sedimentation (Trueman et al., 2006). $(La/Yb)_N$ ratio varies within 1.70–2.54; $(La/Sm)_N$ ratio varies within 1.03–1.57. Apparently, sorption processes were leading in REE fractionation. This supposition is also verified by poorly established tetrad-effect of lanthanoids for the third tetrad (Table 6, Fig. 11). Some samples exhibit the tetrad effect close to the threshold of statistical significance for 3 tetrad, its t-values are close to M-type. It maximal variations are characteristic for horizons of paleosols. Usually a W-type tetrad effect indicates the REE dissolution, while the M-type indicate the REE association with a solid phase (Masuda et al., 1987).

8. Conclusions

The detail multidisciplinary study of the Tologoi section has revealed some sedimentation features and allow to recognize specified location and thickness of fossil soil horizons in the section:

- Four cycles of sedimentation were recognized within Tologoi 2 and Tologoi 3 units, each cycle terminated with formation of soil horizons. The soil horizon in the lower part of the section (Tologoi 1 unit) (2900–3000 cm) also reflects the end of sedimentation cycle.
- During the sedimentation time, the climate changed cyclically: humidification periods were replaced by the arid epochs of different intensity and duration.
- The sedimentary material arrived to the sedimentation site from the nearest source. During the warming stages and formation of soil horizons prevaled the remote sources of sedimentary material. The periods of more intense pedogenic processes were dominated by the biochemical post-sedimentation transformations of in *situ* sediments observed in the change of their chemical composition.
- The most humid conditions and activation of weathering and leaching processes are established for the paleosoil horizons occurring at depth 1290–1500 cm and 2900–3000 cm.

Acknowledgments

The research is supported by the Russian Foundation for Basic Research (projects no. 15-05-01858, 16-05-00586, 18-05-00215)), the Russian Science Foundation (project no. 16-17-10079 (chemical analysis, paleontology)) and Integration Project No. 0341-2016-001. The study was conducted using the research facilities of the Center for Geodynamics and Geochronology at the Institute of the Earth's Crust SB RAS, Irkutsk, Russia. M. A. Erbajeva thanks Prof. W. Zech for the professional assistance.

Appendix A. Supplementary data

Supplementary data associated with this article can be found, in the online version, at https://doi.org/10.1016/j.quaint.2018.11.004.

References

Alexeeva, N.V., 2005. Environmental Evolution of Late Cenozoic of West Transbaikalia (Based on Small Mammal Fauna). GEOS, Moscow, pp. 141 (in Russian).
Alexeeva, N.V., Erbajeva, M.A., 2000. Pleistocene permafrost in western Transbaikalia. Quat. Int. 68–71, 5–12.
Alexeeva, N.V., Erbajeva, M.A., 2005. Changes in the fossil mammal faunas of western Transbaikalia during the pliocene-pleistocene boundary and the early-middle Pleistocene transition. Quat. Int. 131, 109–115.
Alexeeva, N.V., Erbajeva, M.A., Khenzykhenova, F.I., 2014. *Lasiopodomys brandti* in Pleistocene of Transbaiklia and adjacent territories: distribution area evolutionary development in context of global and regional events. Quat. Int. 355, 11–17.
Andreeva, D.B., Leiber, K., Glaser, B., Hambach, U., Erbajeva, M., Chimitdorzhieva, G.D., Tashak, V., Zech, W., 2011. Genesis and properties of black soils in Buryatia, southern Siberia, Russia. Quat. Int. 243, 313–326.
Balashov, YuA., 1976. Geokhimiya Redkozemel'nykh Elementov (Geochemistry of Rare Earth Elements). Nauka, Moscow, pp. 268 (in Russian).
Bazarov, D.B., 1968. The Quaternary Deposits and the Main Stages of Selenginskoye Midland Development. Russian Academy of Sciences, Siberian Branch, Ulan-Ude, pp. 166 (in Russian).
Berezin, P.N., 1983. Osobennosti raspredeleniya granulometricheskikh elementov pochv i pochvoobrazuyushchikh porod. Pochvovedenie 2, 64–72 (in Russian).
Bibikova, V.N., Vereshchagin, N.K., Garutt, V.E., et al., 1953. New data on quaternary fauna of Transbaikalia (oshurkovo, tologoi). Materials and investigations on archaeology of the USSR 39, 26–39 (in Russian).
Blott, S.J., Pye, K., 2001. GRADISTAT: a grain size distribution and statistics package for the analysis of unconsolidated sediments. Earth Surf. Process. Landforms 26, 1237–1248.
Cohen, K.M., Gibbard, P.L., 2016. Global Chronostratigraphical Correlation Table for the Last 2.7 Million Years, V. 2016a. Cambridge: Subcommission on Quaternary Stratigraphy. International Commission on Stratigraphy Retrieved from. http://www.stratigraphy.org/index.php/ics-chart-timescale/.
Cox, R., Lowe, D.R., Cullers, R.L., 1995. The influence of sediment recycling and basement composition on evolution of mudrock chemistry in southwestern United States. Geochem. Cosmochim. Acta 59, 2919–2940.
Dia, A., Gruau, G., Olivié-Lauquet, G., Riou, C., Molénat, J., Curmi, P., 2000. The distribution of rare earth elements in groundwaters: assessing the role of sourcerock composition, redox changes, and colloidal particles. Geochem. Cosmochim. Acta 64, 4131–4152.
Enikeev, F.I., 2008. The late cenozoic of northern Transbaikalia and paleoclimates of southern east siberia. Russ. Geol. Geophys. 49 (8), 602–610.
Enikeev, F.I., Potemkina, V.I., Staryshko, V.E., 2013. Stratigrafiya I Evolyutsiya Klimata I Rastitel'nosti Pozdnego Kainozoya Severnogo Zabaikal'ya. GEO, Novosibirsk, pp. 131 (In Russian).
Erbajeva, M.A., 1970. The History of the Anthropogene Lagomorph and Rodent Faunas of Selenginskoye Midland. Nauka, Moscow, pp. 132 (in Russian).
Erbajeva, M.A., Alexeeva, N.V., 2000. Pliocene and Pleistocene biostratigraphic succession of Transbaikalia with emphasis on small mammals. Quat. Int. 68–71, 67–75.
Erbajeva, M.A., Karasev, V.V., Alexeeva, N.V., 2005. New evidences on the pliocene-pleistocene stratigraphy of Transbaikalia. Russ. Geol. Geophys. 46 (4), 414–423.
Erbajeva, M.A., Khenzykhenova, F.I., Alexeeva, N.V., 2013. Aridization of the Transbaikalia in the context of global events during the Pleistocene and its effect on the evolution of small mammals. Quat. Int. 284, 45–52.
Fedo, C.M., Nesbitt, H.W., Young, G.M., 1995. Unraveling the effects of potassium metasomatism in sedimentary rocks and paleosols, with implications for paleoweathering conditions and provenance. Geology 23, 921–924.
Folk, R.L., Ward, W.C., 1957. Brazos River bar: a study in the significance of grain size parameters. J. Sediment. Petrol. 27, 3–26.
Gnibidenko, Z.N., Erbajeva, M.A., Pospelova, G.A., 1976. Paleomagnetism and biostratigraphy of some late cenozoic sediments of western Transbaikalia. In: Paleomagnetism of Mezozoic and Cenozoic of Siberia and Far East, pp. 76–95 (in Russian).
Gradzin'skii, R., Kostetskaya, A., Radomskii, A., Unrug, R., 1980. Sedimentologiya. Nedra, Moscow, pp. 640 (in Russian).
Grazhdankin, D.V., Maslov, A.V., 2012. Litokhimicheskie osobennosti primitivnykh paleopochv v razreze srednei chasti bederyshinskoi podsvity zil'merdakskoi svity verkhnego rifeya na yuzhnoi okraine g. Min'yar. Trudy IGG UrO RAN 159, 77–84 (in Russian).
Gromet, L.P., Dymek, R.F., Haskin, L.A., Korotev, R.L., 1984. The North American Shale Composit: its composition, major, and trace element characteristics. Geochem. Cosmochim. Acta 48, 2469–2482.
Irber, W., 1999. The lanthanide tetrad effect and its correlation with K/Rb, Eu/Eu*, Sr/Eu, Y/Ho, and Zr/Hf of evolving peraluminous granite suites. Geochem. Cosmochim. Acta 63, 489–508.
Ivanova, V.V., Shchetnikov, A.A., Filinov, I.A., Veshcheva, S.V., Kazansky, A.Y., Matasova, G.G., 2016. Lithogeochemistry of rocks of the upper Neopleistocene Ust-Oda reference section in the Irkutsk amphitheater of the Siberian platform. Lithol. Miner. Resour. 51 (3), 179–194.
Kalinin, P.I., Alekseev, A.O., Savko, A.D., 2009. Lessy, Paleopochvy I Paleogeografiya Kvartera Yugo-vostoka Russkoi Ravniny. Voronezhskii gosudarstvennyi universitet, Voronezh (in Russian).
Kuzmin, M.I., Yarmoluyk, V.V., 2006. Geological forcing of climate in Earth'. Russian Journal of Geology and Geophysics 47 (1), 7–25 (in Russian).
Logatchev, N.A., Lomonosova, T.K., Klimanova, V.M., 1964. Cenozoic Deposits of the Irkutsk Amphitheatre. Nauka, Moscow, pp. 195 (in Russian).
Maslov, A.V., 2005. Osadochnye Porody: Metody Izucheniya I Interpretatsii Poluchennykh Dannykh (Sedimentary Rocks: Methods for the Study and Interpretation of Obtained Data). UGGU, Yekaterinburg, pp. 289 (in Russian).
Masuda, A., Ikeuchi, Y., 1979. Lanthanide tetrad effect observed in marine environment. Geochem. J. 13, 19–22.
Masuda, A., Kawakami, O., Dohmoto, Y., Takenaka, T., 1987. Lanthanide tetrad effects in nature: two mutually opposite types, W and M. Geochem. J. 21, 119–124.
McLennan, S.M., 1994. Rare earth element geochemistry and the "tetrad" effect. Geochem. Cosmochim. Acta 58, 2025–2033.
Monecke, T., Kempe, U., Monecke, J., et al., 2002. Tetrad effect in rare earth element distribution patterns: a method of quantification with application to rock and mineral samples from granite-related rare metal deposits. Geochem. Cosmochim. Acta 66, 1185–1196.
Nesbitt, H.W., Young, G.M., 1982. Early Proterozoic climates and plate motions inferred from major element chemistry of lutites. Nature 299, 715–717.
Nesbitt, H.W., Young, G.M., 1984. Prediction of some weathering trends of plutonic and volcanic rocks based on thermodynamic and kinetic considerations. Geochem. Cosmochim. Acta 48 (7), 1523–1534.
Pillans, B., Gibbard, P., 2012. The Quaternary period. In: Gradstein, F., Ogg, J., Schmitz, M., Ogg, G. (Eds.), The Geological Time Scale 2012. Elsevier, Amsterdam, pp. 979–1010.
Prokopenko, A.A., Karabanov, E.B., Williams, D.F., Kuzmin, M.M., Khursevich, G.K., Gvozdkov, A.A., 2001. The link between tectonic and paleoclimatic events at 2.8-2.5 Ma BP in the Lake Baikal region. Quat. Int. 80–81, 37–46.
Raukas, A.V., 1981. Donnye Otlozheniya Pskovsko-chudskogo Ozera. 1981. Akademiya Nauk Estonskoi SSR, Tallin, pp. 160 (in Russian).
Ravsky, E.I., 1972. Sedimentaion and Climate of Inner Asia during the Anthropogene. Nauka, Moscow, pp. 160 (in Russian).
Ravsky, E.I., Alexandrova, L.P., Vangengeim, E.A., Gerbova, V.G., Golubeva, L.V., 1964. Anthropogene Deposits of Southern East Siberia. Nauka, Moscow, pp. 280 (in Russian).
Retallack, G.J., 2001. Soils of the Past: an Introduction to Paleopedology, second ed. Blackwell, Oxford, pp. 600.
Retallack, G.J., 2007. 5.18 - soils and global change in the carbon cycle over geological time. In: Holland, H.D., Turekian, K.K. (Eds.), Treatise on Geochemistry. Elsevier, Oxford, pp. 1–28.
Sheldon, N.D., 2006. Abrupt chemical weathering increase across the Permian–Triassic boundary. Palaeogeogr. Palaeoclimatol. Palaeoecol. 231, 315–321.
Sheldon, N.D., Tabor, N.J., 2009. Quantitative paleoenvironmental and paleoclimatic reconstruction using paleosols. Earth Science Review 95, 1–52.
Sochava, V.E. (Ed.), 1967. Transbaikalia Atlas. Principal Managing Department on Geodesy and Cartography, Moscow, pp. 176 (in Russian).
Tarasov, P., Bezrukova, E., Krivonogov, S., 2009. Late Glacial and Holocene changes in

vegetation cover and climate in southern Siberia derived from a 15 kyr long pollen record from Lake Kotokel. Clim. Past 5, 285–295.
Taylor, S.R., McLennan, S.M., 1985. The Continental Crust; its Composition and Evolution; an Examination of the Geochemical Record Preserved in Sedimentary Rocks. Blackwell, Oxford, pp. 312.
Trueman, C.N., Behrensmeyer, A.K., Potts, R., Tuross, N., 2006. High-resolution records of location and stratigraphic provenance from the rare earth element composition of fossil bones. Geochem. Cosmochim. Acta 70, 4343–4355.
Vangengeim, E.A., Beliajeva, YeI., Dubrovo, I.A., Garutt, V.Ye, Zazhigin, V.S., 1966. Mammals of the Eopleistocene Key Sections of the Western Transbaikalia. Nauka, Moscow, pp. 163 (in Russian).
Vogt, T., Erbajeva, M., Vogt, H., 1995. Premières preuves de conditions périglacières au Pléistocène inférieur en Transbaikalie (Sibérie, Russie). Comptes Rendus de l'académie des Sciences de Paris, Séries A 320, 861–866.
Yudovich, YuE., Ketris, M.P., 2000. Osnovy Litokhimii (Principles of Lithochemistry). Nauka, St. Petersburg, pp. 479 (in Russian).
Zech, W., Andreeva, D., Zech, M., Bliedtner, M., Glaser, B., Hambach, U., Erbajeva, M., Zech, R., 2017. The Tologoi Record: a terrestrial key profile for the reconstruction of Quaternary environmental changes in semiarid Southern Siberia. In: Abstract Book, the 3rd Asian Association for Quaternary Research (ASQUA) Conference. NRF, Lotte City, Republic of Korea, pp. 13.